Sub-lethal concentrations of artemisinin alter pH of the digestive vacuole of the malaria parasite, *Plasmodium falciparum*

Ibrahim, N., Roslee, A., Azlan, M. and Abu-Bakar, N.*
School of Health Sciences, Health Campus, Universiti Sains Malaysia, 16150 Kubang Kerian, Kelantan, Malaysia
*Corresponding author e-mail: natashaa@usm.my

Abstract. An appropriate pH maintenance within a membrane-enclosed organelle is vital for the occurrence of biological processes. Artemisinin (ART), a potent antimalarial drug has been reported to target the digestive vacuole (DV) of *Plasmodium falciparum*, which might alter the pH of the organelle, thereby impairing the hemoglobin degradation and subsequent heme detoxification. Hence, a flow cytometry-based technique using fluorescein isothiocyanate-dextran (FITC-dextran) as a ratiometric pH probe was employed to measure the pH of the DV of the malaria parasite treated with ART. Based on the pH calibration curve generated, the steady-state pH of the acidic DV of the non-treated parasites was 5.42 ± 0.11, indicating that FITC-dextran is suitable for detection of physiological pH of the organelle. The alteration of the DV pH occurred when the parasites were treated with ART even at the sub-lethal concentrations (15 and 30 nM) used. The similar effect was shown by the parasites treated with a standard proton pump inhibitor, concanamycin A. This suggests that ART might have altered the DV pH at lower levels than the level needed to kill the parasite. This study has important implications in designing new ART treatment strategies and in generating new endoperoxide-based antimalarial drugs pertaining to the interruption of the pH regulation of the malaria parasite's DV.

INTRODUCTION

Malaria is a global health issue. It continues to be a constant threat to humans, causing 219 million malaria cases and 435 000 malaria deaths worldwide in 2017 (World Health Organization, 2018). The disease is transmitted through the bite of infected female *Anopheles* mosquitoes and its clinical manifestations are caused by the blood stage *Plasmodium* parasites (Josling & Llinas, 2015). To date, the treatment for malaria still relies on antimalarial drugs due to the lack of available effective vaccines (Moorthy & Hill, 2018).

Artemisinin-based combination therapies are recommended as a first-line treatment for uncomplicated malaria (World Health Organization, 2018). Artemisinin (ART), which is derived from a Chinese medicinal plant, *Artemisia annua* has a superior activity against blood stage parasites (Mohd-Zamri *et al.*, 2017) and inhibits the growth of parasites, notably multidrug-resistant *P. falciparum*, more rapidly than other drugs (Sullivan, 2013; Guo, 2016). ART and its derivatives are combined with other partner drugs to increase the efficacy of the treatment and to protect both drugs against resistance (World Health Organization, 2018). The emergence of parasites that are resistant to ART and its derivatives has, however, been reported in Southeast Asia such as in Thailand and Cambodia and manifested clinically as longer parasite clearance time (Hanboonkunupakarn & White, 2016; Fairhurst & Dondorp, 2016). Hence, an intense study should be focused

on determining the precise mechanism of action of ART and its biological targets within the parasite to improve treatment strategies.

The initial key step in the mechanism of action of ART has been proposed to be the activation of the endoperoxide bridge by the interaction with one-electron reducing agents such as ferrous heme and non-heme iron that is available within the parasite's digestive vacuole (DV) (Abu Bakar, 2016; Zhang & Gerhard, 2008; Wang *et al.*, 2015). The process has led to the generation of cytotoxic carbon-centered radicals (Pandey & Pandey-Rai, 2015), which might alkylate proteins essential to parasite functions (Bridgford *et al.*, 2018) such as the translationally controlled tumor protein (TCTP) homolog (Bhisutthibhan & Meshnick, 2001) and the parasite-encoded sarco-endoplasmic reticulum Ca^{2+}-dependent ATPase (SERCA) orthologue (*Pf*ATP6) (Eckstein-Ludwig *et al.*, 2003; Wang *et al.*, 2015). However, the downstream effect of the TCTP alkylation by ART that is responsible for its antimalarial activity remains unclear (Bhisutthibhan & Meshnick, 2001; Li & Zhou, 2010). Many studies also failed to reproduce the proposed antagonistic relationship between ART and thapsigargin, an inhibitor of mammalian SERCA, arguing against the suggestion that the interaction with *Pf*ATP6 accounts for the ART action in the parasite (del pilar Crespo *et al.*, 2008; Hartwig *et al.*, 2009).

A study by Wang *et al.* (2015) identified the cellular localization of AP1, a fluorescent dye-tagged ART, in several parasite compartments such as vacuolar membrane and DV. Of interest, V-type H^+-translocating pyrophosphatase (VP1), which is thought to be responsible for maintaining an acidic DV (Saliba *et al.*, 2003; Segami *et al.*, 2018), was targeted by AP1 (Wang *et al.*, 2015). Besides VP1, there is evidence for the presence on the DV membrane of another H^+ pumping mechanism by V-type H^+-ATPase (Hayashi *et al.*, 2000; Saliba *et al.*, 2003; Ismail *et al.*, 2017). VP1 and V-type H^+-ATPase have been demonstrated to act together to maintain a low internal pH of the DV (Saliba *et al.*, 2003; Marchesini *et al.*, 2000) so that proteolytic enzymes such as aspartic and cysteine proteases (have pH optima in the range 4.5-

5.0) could degrade host cell hemoglobin into amino acids (Goldberg, 2005). Therefore, direct inhibition of the proton pumps might result in DV pH alteration, leading to intense disruption of the hemoglobin degradation pathway and eventually parasite death (Schalkwyk *et al.*, 2010; Hayashi *et al.*, 2000).

In the present study, we provide evidence that ART at sub-lethal concentrations alters the pH of the DV of *P. falciparum*. Sub-lethal concentrations of ART were used to ensure that the DV pH alteration was due to a short pulse of the drug not as a consequence of parasite death due to higher drug concentrations.

MATERIALS AND METHODS

Materials
ART was purchased from Sigma-Aldrich. FITC-dextran (10 kDa) and SYBR Green I (10 000x in DMSO) were purchased from Thermo Fisher.

Parasite culture
Chloroquine-sensitive *P. falciparum* (3D7 strain) was cultured using washed human blood (O^+ type) in serum-free complete culture RPMI 1640 medium (CCM) supplemented with 2 mg/mL glucose (Sigma), 0.025 mg/mL gentamicin (Duopharma), 0.05 mg/mL hypoxanthine and 5 mg/mL Albumax (Gibco) (Abu Bakar, 2015). Ring stage parasites (10-18 hours post-invasion) were synchronized using 5% D-sorbitol treatment at 37°C for 10 minutes. After 24 hours, mature stage parasites (34-42 hours post-invasion) were harvested by magnetic column separation technique (Miltenyi Biotec) to obtain an 8- to 10-hour window.

FITC-dextran incorporation into erythrocytes
FITC-dextran (30 µM loading concentration) was incorporated into erythrocytes using a modified method of Abu Bakar (2015) and Ibrahim & Abu-Bakar (2019). Erythrocytes (400 µL) were lysed in ice-cold hemolysis buffer (900 µL) supplemented with 1 mM Mg-ATP. The cell suspension was incubated for 10 minutes to open the pores

in the plasma membrane for allowing the probe to enter the cells. A volume of 220 µL of resealing buffer A (5 mM sodium phosphate, 700 mM sodium chloride, 100 mM potassium chloride, 27.5 mM glucose, pH 7.4) was added into the cell suspension and incubated at 37°C for 20 minutes. Then, a volume of 8.5 mL of resealing buffer B (10 mM sodium phosphate, 140 mM sodium chloride, 20 mM potassium chloride, 5 mM glucose, pH 7.4) was added into the cell suspension and incubated for another 20 minutes at 37°C. The cell suspension was washed (332 × g, 5 minutes) two times with resealing buffer B and one time with CCM. Resealed erythrocytes incorporated with FITC-dextran were inoculated with synchronized mature stage parasites (36-hour post-invasion) ($\geq$90% purity) and cultured in normal culture conditions (2% hematocrit, 2% parasitemia). The parasite growth and parasitemia were determined by Giemsa-stained thin blood smears.

pH calibration using FITC-dextran
Before the fluorescence intensity of DV-associated FITC-dextran was measured, any fluorescent marker in the cytoplasm of resealed erythrocytes was released by saponin treatment. Trophozoite stage parasites at 34-hour post-invasion (which was at 42-hour post-inoculation) in resealed erythrocytes were permeabilized by brief exposure to 0.035% saponin (an optimized final concentration, w/v sapogenin, pH 7.5, Sigma) at room temperature (Saliba & Kirk, 1999; Abu Bakar, 2015). Saponin-permeabilized parasites were suspended in a medium containing RPMI 1640, 25 mM HEPES, 0.02 mg/mL gentamycin, 0.4 mM hypoxantine and 0.125% albumax, and kept at 37°C until being used.

To generate a pH calibration curve of FITC-dextran, saponin-permeabilized parasites (1.5 x 10^7/mL) were suspended in 20 mM buffer containing 150 mM NaCl (Abu Bakar, 2015). Buffers used were 2-[N-morpholino] ethane sulfonic acid (MES, pH 4.0, 5.5 and 6.0), sodium phosphate (NaH_2PO_4, pH 6.5, 7.0, 7.5 and 8.0) and tris (hydroxymethyl) aminomethane (TRIS, pH 9.0). An ionophore, carbonyl cyanide m-chlorophenylhydrazone (CCCP, from a stock of 10 mM in DMSO, Sigma) was added to a final concentration of 10 ìM to equilibrate the pH of saponin-permeabilized parasites to the pH of external buffers before analysis by flow cytometry.

Flow cytometry analysis was performed on a FACSCanto II (Becton Dickinson). FITC-dextran was excited using a 488 nm argon ion laser and its fluorescence intensity was collected at FITC or green (530 nm) and PE or yellow (585 nm) channels (Abu Bakar, 2015; Ibrahim & Abu-Bakar, 2019). Data were analyzed by FCS Express 5 Flow Cytometry Software (De Novo Software). The population of saponin-permeabilized parasites was gated based on its scatter profile and 10 000 events per sample were collected. An additional gate based on the fluorescence intensity of FITC-dextran at green and yellow channels was established to select saponin-permeabilized parasites that had the DV containing FITC-dextran. Histograms were plotted to obtain the peak of the fluorescence intensity for both green and yellow channels from which ratios of green/yellow fluorescence intensity (R_{gy}) were measured. R_{gy} was plotted as a function of pH in a pH calibration curve of FITC-dextran.

The 4-hour ART pulse assay
The 4-hour pulse with different concentrations of ART was performed using a modified protocol of Klonis *et al.* (2011) and Mohd-Zamri *et al.* (2017). Different concentrations of ART in CCM were prepared in triplicates by serially diluting the highest concentration of ART (1000 nM) across 96-well plates before being added into plates containing synchronized mid ring stage parasites at 10-hour post-invasion (18-hour post-inoculation) (2% hematocrit, 2% parasitemia). Parasites were pulsed with ART for 4 hours, washed and cultured in normal culture conditions for a further 24 hours before being split into two groups. The first group of the parasites was stained with 1x SYBR Green I and analyzed by flow cytometry to assess parasite growth and parasitemia within the same parasite cycle (~24-hour post-treatment). The second

group of the parasites was cultured for an additional 24 hours before staining with SYBR Green I in the next parasite cycle (~48-hour post-treatment) to assess parasite viability.

SBYR Green I was used to monitor parasite growth (intensity) and parasitemia (fraction of parasite-infected erythrocytes) after pulse with ART. A 488 nm argon ion laser was used as an excitation source for SYBR Green I and the fluorescence signal was collected at 530 nm. The population of parasites stained with SYBR Green I was gated based on the scatter and SYBR Green I profile of the cells. A graph was plotted as ART concentration (log) versus parasitemia (at 24- and 48-hour post-treatment). The percentage of parasite growth inhibition was calculated based on the parasitemia at 48-hour post-treatment and plotted as a function of ART concentration (log) to determine the 4-hour pulse 50% inhibitory concentration ($IC_{50\text{-}4 \text{ hours}}$) and sub-lethal concentrations that kill <25% of the parasite population. The sub-lethal concentrations of ART that affected the SYBR Green I staining at 24-hour post-treatment but not the parasitemia at 48-hour post-treatment were employed in the subsequent experiment. The SYBR Green I intensity profiles of the gated populations of the parasites at 24-hour post-treatment are displayed in the histograms.

The effect of sub-lethal ART concentrations on DV pH

Synchronized mid ring stage parasites at 10-hour post-invasion (18-hour post-inoculation) with and without FITC-dextran (2% hematocrit, 2% parasitemia) were pulsed for 4 hours with sub-lethal concentrations of ART and ART concentration near the $IC_{50\text{-}4 \text{ hours}}$. Non-treated parasites and parasites treated with 1000 nM ART were used as negative and positive controls, respectively. Then, parasites were washed and cultured in normal culture conditions for a further 24 hours. The group of parasites without FITC-dextran was split into two aliquots. The first aliquot was stained with 1x SYBR Green I and analyzed by flow cytometry to assess parasite growth and parasitemia within the same parasite cycle

(~24-hour post-treatment), while the second aliquot was cultured for an additional 24 hours before staining with SYBR Green I in the next parasite cycle (~48-hour post-treatment) to assess parasite viability. The group of parasites with FITC-dextran was added with saponin (0.035% w/v) to prepare for saponin-permeabilized parasites for DV pH measurement by flow cytometry within the same parasite cycle (~24-hour post-treatment). The same treatment of 4-hour ART pulse was done on synchronized mid trophozoite stage parasites at 34-hour post-invasion (42-hour post-inoculation) to confirm the DV pH alteration was caused by the sub-lethal concentrations of ART not by a secondary effect of parasite killing. After 4-hour pulse, the parasites were washed and permeabilised with saponin to measure the DV pH using flow cytometry.

RESULTS

FITC-dextran as a pH probe for flow cytometry

In situ pH calibration is needed for flow cytometry as the fluorescence characteristics of FITC-dextran in buffers may be slightly different to those observed when the probe is incorporated into erythrocytes (Bagar *et al.*, 2009). Therefore, a pH calibration curve was constructed by suspending saponin-permeabilized parasites in buffers of different pH in the presence of CCCP to equilibrate the intracellular compartments of the parasites to the external buffers of known pH. Ratios (R_{gy}) of the FITC-dextran fluorescence intensity collected at green and yellow channels by flow cytometry were calculated from three independent experiments and plotted as a function of pH as shown in Figure 1A.

The acid-base transition was observed by the increase in R_{gy} values with increasing pH. FITC-dextran with a pK_a value of 6.0 (Figure 1A, the inflexion point in the curve) can be used to distinguish between acidic and basic compartments. The DV within parasite-infected erythrocytes suspended in a buffer without CCCP shows a R_{gy} value of 5.31 ± 0.2, corresponding to the DV pH
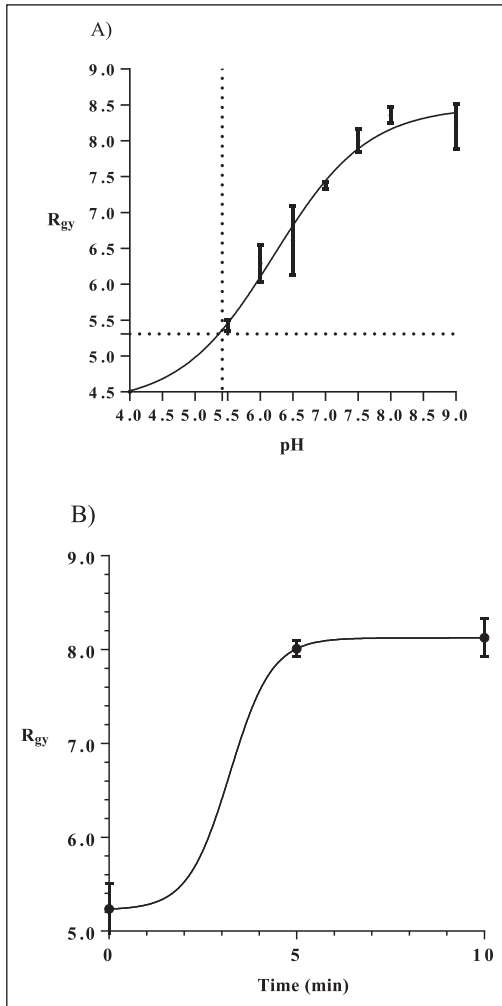
Figure 1. FITC-dextran as a pH probe for flow cytometry.
A) A pH calibration curve was generated using FITC-dextran in saponin-permeabilized erythrocytes. The pH of the DV of non-CCCP treated parasites was determined from the curve (shown by dotted lines). B) The increase in R_{gy} values after 5 minutes of the incubation with concanamycin A (75 nM) indicates the alkalinization of the DV. The data are expressed as mean ± SEM derived from three independent experiments done in triplicates (n=3). The dose-response curves were fitted by non-linear regression with GraphPad Prism (version 7).

value of 5.42 ± 0.11 (Figure 1A, dotted line). This value is comparable to the DV pH measured by Hayward *et al.* (2006), Abu Bakar (2015) and Ibrahim & Abu-Bakar (2019). When concanamycin A (75 nM), a proton pump inhibitor (Figure 1B) was added into the parasite suspension, the increase

in R_{gy} values was observed, indicating an alkalinizing process of the DV. The complete alkalinization of the DV was achieved after 10 minutes (R_{gy} = 8.13 ± 0.15; DV pH = 7.7 ± 0.2). The results confirm that the R_{gy} measurement can distinguish between FITC-dextran located in the acidic DV and that present in a neutral or an alkaline environment.

The short 4-hour ART pulse produces different parasite populations
In the present study, mid ring stage parasites (18-hour post-inoculation) were exposed to a 4-hour pulse with a range of ART concentrations (0-1000 nM) to mimic the *in vivo* effect of the short half-life drug. The SYBR Green I profiles of the parasite populations were monitored to determine parasite growth and parasitemia after ART treatment within the same cycle (~24-hour post-treatment) and during the next cycle (~48-hour post-treatment). Since the host erythrocytes are absence of nucleic acids, SYBR Green I, which binds to double stranded DNAs of the parasites, can readily distinguish between uninfected, ring stage- and mature stage-infected erythrocytes by flow cytometry (Bei *et al.*, 2010).

During the cycle of the drug pulse (~24-hour post-treatment), the parasitemia of treated groups remained constant (Figure 2A, circles), however a drug concentration-dependent decrease in the parasitemia (Figure 2A, triangles) was observed during the next cycle of the drug pulse (~48-hour post-treatment) with an $IC_{50-4 \ hours}$ value of 50.63 ± 1.08 nM obtained from the graph of the percentage of parasite growth inhibition (Figure 2B, dotted line). There was a drug concentration-dependent decrease in the SYBR Green I intensity during the same cycle of the drug pulse, indicating the presence of different parasite populations (Figure 2C). Interestingly, the parasites that survived the treatment with ART concentrations less than the $IC_{50-4 \ hours}$ at 15.6 nM (Figure 2C, green curve) and 31.3 nM (Figure 2C, purple curve), showed a significant slowing of the growth compared to the non-treated parasites (Figure 2C, black curve) as judged by the lower SYBR Green I intensity. The delay in
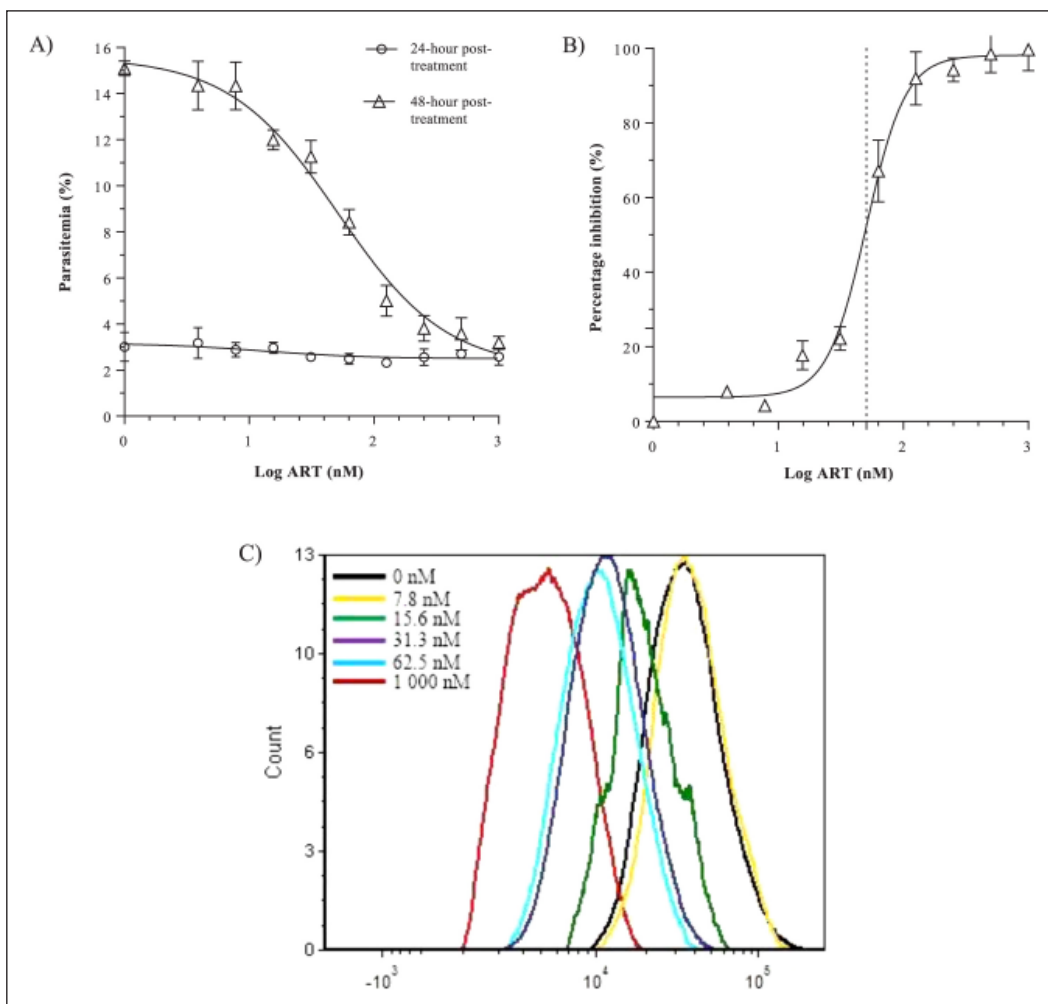
Figure 2. The 4-hour ART pulse assay produces different parasite populations.
Ring stage parasites were pulsed with different ART concentrations for 4 hours, washed and cultured for a further 24 hours. A) The parasites were labelled with SYBR Green I and analyzed by flow cytometry 24 hours (circles) and 48 hours (triangles) later to determine the parasitemia. B) The 4-hour pulse 50% inhibitory concentration ($IC_{50\text{-}4 \text{ hours}}$) of ART was determined for the percentage of parasite growth inhibition curve (dotted lines). C) The SYBR Green I profiles of non-treated and treated parasites at 24-hour post-treatment measured using flow cytometry. Error bars indicate means ± SEM derived from three independent experiments done in triplicates (n=3). The dose-response curves were fitted by non-linear regression with GraphPad Prism (version 7).

parasite growth was apparent by the smaller size of the trophozoites (Figure 3A, the third and fourth panels from the left) than that of the non-treated trophozoites observed in Giemsa-stained thin blood smears (Figure 3A, the first panel from the left). The highest SYBR Green I intensity was exhibited by the non-treated parasites (Figure 2C, black curve) and the parasites treated with the lowest drug concentration examined (7.8 nM) (Figure 2C, yellow curve). Most of the parasites in these groups progressed from rings to large trophozoites (Figure 3A, the first and second panels from the left). The pronounced decrease (10-fold) in staining was observed by the parasites treated with the highest drug concentration (1000 nM) (Figure 2C, red curve). The growth was completely inhibited as shown by the presence of earlier rings that did not develop
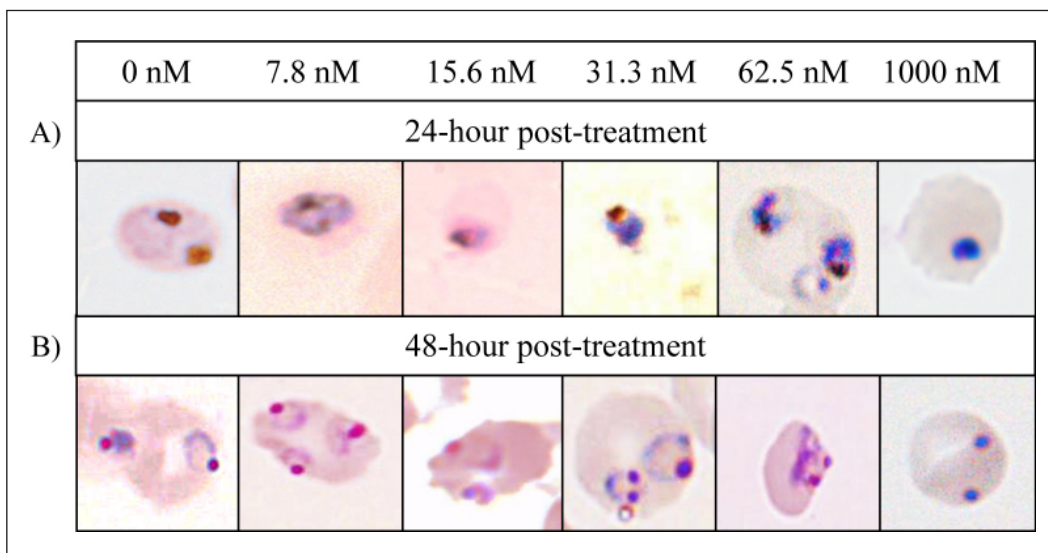
Figure 3. The morphology of *P. falciparum* pulsed for 4 hours with ART.
The Giemsa staining of non-treated and treated parasites observed at (A) 24-hour post-treatment to examine the parasite growth and development within the same cycle of the drug pulse and at (B) 48-hour post-treatment to examine the parasite growth and development during the next cycle. The experiments were conducted in three different occasions done in triplicates.

to trophozoites compared to the non-treated parasites (Figure 3A, the first panel for the right).

The viability of the treated parasites after 48-hour treatment (the next cycle of the drug pulse) was also confirmed by monitoring the entry of the parasites into the next cycle by flow cytometry and by examining parasite morphology by Giemsa analysis. The appearance of new ring stage parasites in sub-lethal ART concentration-treated groups (Figure 3B, the third and fourth panels from the left) indicates the development of the parasites into a new cycle as evidence be the increasing parasitemia (Figure 2A, triangles). Meanwhile, the parasites treated with the higher concentrations did not grow and appeared as the earlier rings with pyknotic morphology as marked by constant or unchanged parasitemia compared to the non-treated parasites (Figure 2A, triangles).

Therefore, from the above analyses, ART concentrations less than $IC_{50\text{-}4\ hours}$ value (15 and 30 nM) were chosen and employed in the subsequent experiment. These sub-lethal concentrations caused <25% parasite death and produced a population that likely represents a viable population whose growth had been retarded. The SYBR Green I staining is capable of distinguishing between non-viable parasites with very low intensity and viable parasites with intensity that is moderately decreased.

Sub-lethal concentrations of ART alter the DV pH

The DV pH measurement in saponin-permeabilized parasites after pulse for 4 hours with the sub-lethal ART concentrations (15 and 30 nM) and the ART concentrations that kill more than 50% parasite population (60 and 1000 nM) was performed 24 hours after treatment. To confirm only viable parasite populations from sub-lethal concentration-treated groups were subjected to DV pH measurement, the SYBR Green I intensity profiles within the same cycle of the drug pulse (24-hour post-treatment) were evaluated. As for the parasites growing in the erythrocytes, no change in the parasitemia was observed (Figure 4A, circles), but the SYBR Green I intensity revealed different populations of the parasites (Figure 4B). At 15 and 30 nM (Figure 4Bii, yellow and red curve), a moderate decrease in SYBR Green I intensity staining of the parasite populations
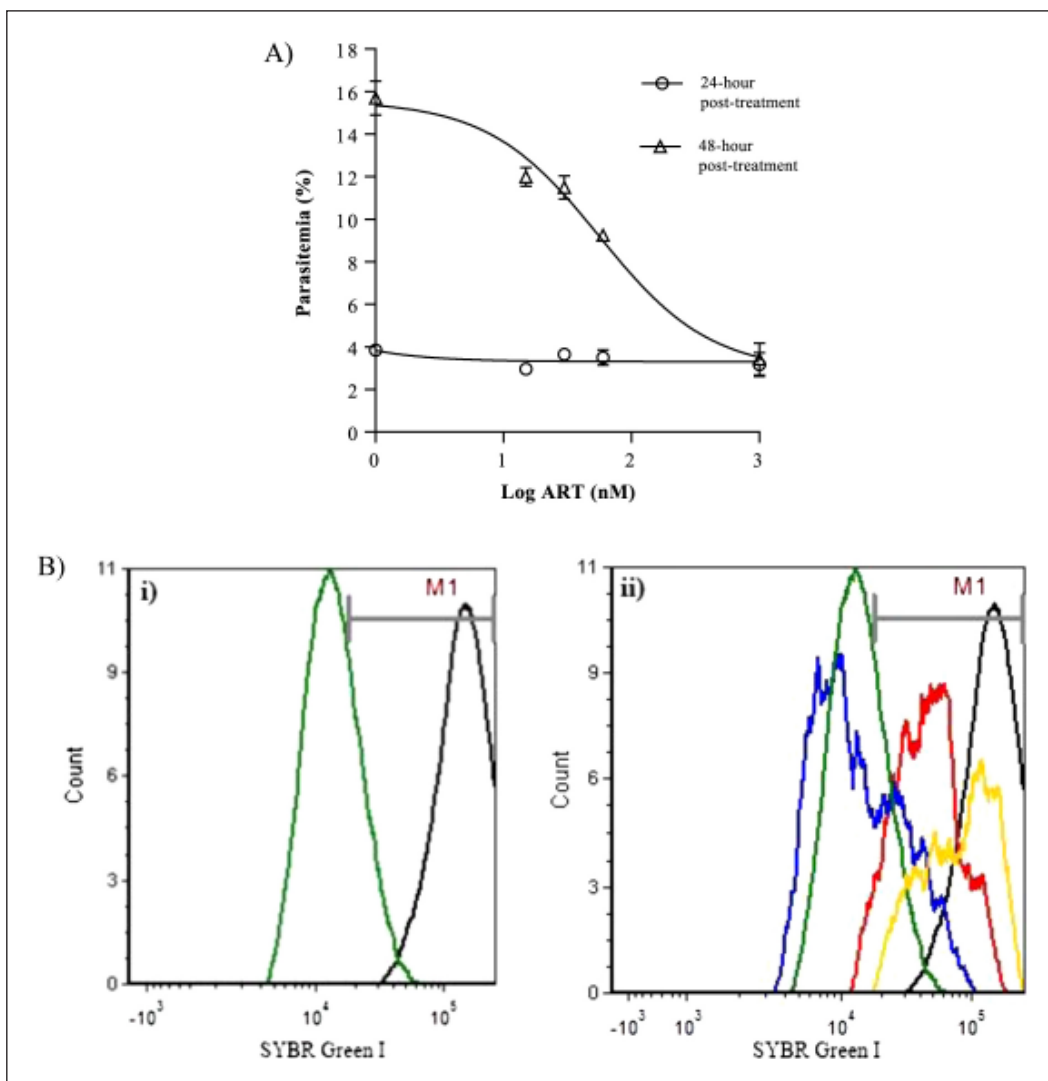
Figure 4. Sub-lethal concentrations of ART delayed the parasite development.
The parasites were pulsed for 4 hours with the sub-lethal ART concentrations. A) The parasitemia was measured 24 hours (circles) and 48 hours (triangles) after treatment. B) The staining profiles of SYBR Green I of the parasite populations 24 hours after treament in the absence (black curve), lethal (60 and 1000 nM, blue and green curves) and sub-lethal (15 and 30 nM, yellow and red curves) concentrations of ART. The grey bar (M1) represents the viable parasite population, which is generated from the different populations of negative control and positive controls (0 and 1000 nM). Error bars indicate means ± SEM derived from three independent experiments done in triplicates (n=3). The dose-response curves were fitted by non-linear regression with GraphPad Prism (version 7).

was observed. These corresponded to the viable parasite populations that were consistent with the viable parasite population of the non-treated group (Figure 4Bi and ii, black curve). The viable gate indicated by the grey bar in Figure 4Bi and ii was used to select the viable parasite populations where the treatments affected the staining of SYBR Green I at 24 hours but not the parasitemia at 48 hours (Figure 4A, triangles). Again, the low intensity population (1000 nM ART) (Figure 4Bi and ii, green curve) correlated with the non-viable parasite population that did not survive into the next cycle (Figure 4A, triangles).
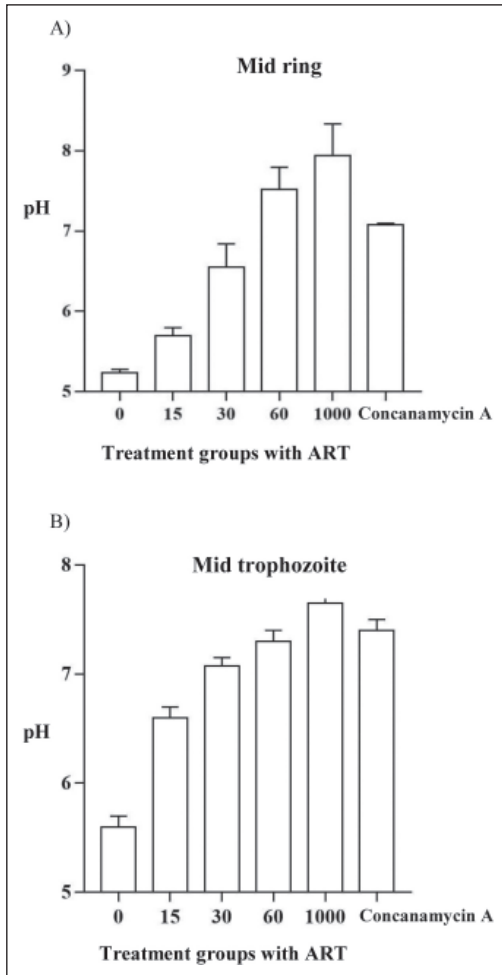
Figure 5. Sub-lethal ART concentrations altered the DV pH.

A) Mid ring and B) mid trophozoite stage parasites were pulsed with 15 and 30 nM (sub-lethal concentrations), 60 nM (concentration near the $IC_{50\text{-}4\ hours}$), 1000 nM (positive control) and no ART (negative control). A standard proton pump inhibitor, concanamycin A was also used in the treatment. The data are expressed as mean ± SEM from three independent experiments done in triplicates. The bar graph was generated using GraphPad Prism (version 7).

The pH of the DV of the viable parasites pulsed with 15 and 30 nM ART for 4 hours was 0.49 (DV pH = 5.7 ± 0.1) and 1.56 pH unit higher (DV pH = 6.77 ± 0.48) than that of the non-treated parasites (DV pH = 5.21 ± 0.04) (Figure 5). The transition of the DV pH from acidic to basic was observed in the population of viable parasites treated with ART concentration near the $IC_{50\text{-}4\ hours}$ (60 nM) (DV pH = 7.48 ± 0.28). The similar results were observed in the non-viable parasite populations treated with 1000 nM ART (DV pH = 7.83 ± 0.32) and the standard proton pump inhibitor, concanamycin A (DV pH = 7.08 ± 0.02).

For the treatment of 4-hour ART pulse on trophozoite stage parasites, the pH of the DV of the viable parasites pulsed with 15 and 30 nM ART was 1 (pH = 6.6 ± 0.1) and 1.48 pH unit higher (pH = 7.1 ± 0.08) than that of the non-treated parasites (pH = 5.6 ± 0.1) (Figure 5B). The transition of the DV pH from acidic to basic was observed in the population of viable parasites treated with ART concentration near the $IC_{50\text{-}4\ hours}$ (60 nM) (pH = 7.3 ± 0.1). Similar results were observed in the non-viable parasite populations treated with 1000 nM ART (pH = 7.65 ± 0.15) and the standard proton pump inhibitor, concanamycin A (pH = 7.4 ± 0.1) (Figure 5B). Therefore, the sub-lethal concentrations of ART altered the pH of the DV of the malaria parasites treated for 4 hours at mid ring and trophozoite stages.

DISCUSSION

During the 48 hours intraerythrocytic cycle, *P. falciparum* develops through the stages of ring, trophozoite and merozoite-containing schizont (Gruring *et al.*, 2010). After the erythrocyte rupture, the parasite continues the cycle by invading a new erythrocyte. As the parasite develops in the erythrocyte, it ingests and degrades hemoglobin in the acidic DV, which reaches a peak in the stage of mid trophozoites (Abu Bakar *et al.*, 2010; Grimberg *et al.*, 2008). ART activated by heme or ferrous iron that is available in the DV has been reported to cause the disruption of the DV membrane (del pilar Crespo *et al.*, 2008; Hartwig *et al.*, 2009), which likely to target proteins such proton pumps located on the DV membrane. But, it is still not clear if it is a direct effect or a consequence of parasite death. To examine the downstream consequence of ART action, the pH of the DV of the parasites treated with the sub-lethal concentrations of the drug was measured.

9

In this study, FITC-dextran as a ratiometric probe of pH of the DV in the trophozoite stage parasites was used. Flow cytometry-based measurements were carried out in the parasites isolated from their host erythrocytes by saponin permeabilization of the erythrocyte membrane. This was to measure the FITC-dextran fluorescence signal directly from the DV based on the detection of its fluorescence intensity at two emission wavelengths. This method is more reliable than a single detection of wavelength due to the ability in compromising the effect of photobleaching, optical path length and local probe concentration (Han & Burgess, 2010). A calibration procedure, which included the use of an ionophore, CCCP was devised to enable quantitative estimation of the pH from the FITC-dextran distribution. The pH-dependent fluorescence of FITC-dextran exhibited a sigmoidal response over a pH range of 4.0 to 9.0. From the generated pH calibration curve, the pK_a of the dye was ~6.0, which is approximately similar to the pK_a of FITC-dextran measured by Abu Bakar (2015), Marchetti *et al.* (2009) and Ibrahim & Abu-Bakar (2019). Based on this profile, FITC-dextran is capable of distinguishing between acidic, basic and neutral compartments and can be used to measure the acidic DV pH at pH values less than 6. The generated calibration curve was validated by measuring the pH of the DV of non-treated parasites in which the DV had an acidic pH. The similar result was shown by other researchers (Kuhn *et al.*, 2007; Hayward *et al.*, 2006). The use of concanamycin A, a specific H$^+$-ATPase inhibitor, resulted in the alkalinization of the DV pH. This observation is consistent with the presence on the DV membrane of a functional proton pump (Schalkwyk *et al.*, 2013; Saliba *et al.*, 2003).

The 48 hours antimalarial drug inhibition assay, which determines the inhibitory concentration that kills 50% of the parasite population (IC$_{50}$) is commonly used to screen the activity of drugs (Smilkstein *et al.*, 2004). However, this traditional assay could not identify the significant difference in the IC$_{50}$ of ART (Dondorp *et al.*, 2009; WHO, 2010; Dondorp *et al.*, 2010), although the delay in

parasite clearance times has been observed in blood samples of patients treated with ART (Enserink, 2010; Eastman & Fidock, 2009). At present, drug pulse inhibition assays at synchronized ring stages have been preferred by researchers to separate parasite populations showing a phenotype of delayed parasite clearance rate in order to elucidate the precise mechanism of ART action (Klonis *et al.*, 2011; Sullivan, 2013; Chotivanich *et al.*, 2014; Xie *et al.*, 2014).

In this work, we designed the experiments to focus on the events in the mid ring to mid trophozoite stages of infection. The synchronized mid ring stage parasites (18-hour post-inoculation) were pulsed for 4 hours with the sub-lethal ART concentrations, washed and cultured in normal culture conditions for a further 24 hours. Next, the trophozoite stage parasites were isolated by saponin to measure the FITC-dextran fluorescence signal directly from the DV for pH measurement. We found that the sub-lethal ART concentrations produced different parasite populations, which had a delayed development but still caused an increase in parasitemia in the next parasite cycle of the drug pulse. This finding is in agreement with the previous works done by Klonis *et al.* (2011), Chotivanich *et al.* (2014) and Xie *et al.* (2014). This delayed but viable parasite population also exhibited an increase in DV pH, indicating the alteration of the DV pH had occurred even at the sub-lethal ART concentrations that did not kill the parasites. To further confirm that the pH alteration of the DV was due to a direct result of ART treatment and not due to a secondary effect of the drug, we performed the DV pH measurement using synchronized mid trophozoite stage parasites pulsed with ART for 4 hours. The short 4-hour pulse with the sub-lethal concentration of ART (15 nM) on the mid ring and mid trophozoite stages caused 0.49 and 1 DV pH unit higher, respectively, than the DV of untreated parasites. According to Eriksson *et al.* (2017), the increase of only a few tenths of a pH unit can have a major impact on the lysosomal function in which the organelle needs to maintain an acidic pH condition as in the DV for the optimal activity of proteases.

The response of the DV pH alteration caused by the short pulse with the sub-lethal ART concentrations was confirmed by the treatment of the parasites with a standard proton pump inhibitor, concanamycin A. It caused an alkalinization of the DV, suggesting that the DV's proton pumps may be active *in situ* at least under the conditions employed in this experiment. Therefore, the inhibition of the proton pumps, which have a major role in maintaining the acidic DV pH has become a possible cause for ART action. The DV pH alteration caused by ART has been shown in the previous study by del Pilar Crespo *et al.* (2008). The alteration of the cellular distribution of the pH probe (LysoSensor Blue DND-192) in the DV suggests early disruption of the pH gradient. The disruption of pH gradient is also related to the effect of ART, which caused rapid depolarization of the DV membrane by disturbing its electrochemical potentials (Antoine *et al.*, 2014). The generated proton potential across the plasma membrane of *P. falciparum* by V-type H^+-ATPase is around -95 mV (Allen & Kirk, 2004), which is responsible for the movement of protons across the membrane. This may suggest that depolarization of the DV membrane can cause the pH alteration in the DV through the direct inhibition of the V-type H^+-ATPase, which is also identified as the target of ART using the ART activity-based protein profiling probes in the click chemistry studies (Ismail *et al.*, 2016). We concluded that the pH alteration in the DV may be a primary consequence of ART antimalarial action that can disturb physiological activities in the DV and thus leads to the parasite death.

REFERENCES

Abu Bakar, N. (2016). Non-heme (Inorganic) iron (II) is a possible primary activator of artemisinin in *Plasmodium falciparum*-infected erythrocytes. *Health and the Environmental Journal* **7**(1): 25-42.

Abu Bakar, N. (2015). Measuring pH of the *Plasmodium falciparum* digestive vacuole by flow cytometry. *Tropical Biomedicine* **32**(3): 485-493.

Abu Bakar, N., Klonis, N., Hanssen, E., Chan, C. & Tilley, L. (2010). Digestive vacuole genesis and endocytic processes in the early intraerythrocytic stages of *Plasmodium falciparum*. *Journal of Cell Science* **123**: 441-450.

Allen, R.J.W. & Kirk, K. (2004). The membrane potential of the intraerythrocytic malaria parasite *Plasmodium falciparum*. *The Journal of Biological Chemistry* **279**(12): 11264-11272.

Antoine, T., Fisher, N., Ameweu, R., O'Neill, P.M., Ward, S.A. & Biagini, G.A. (2014). Rapid kill of malaria parasites by artemisinin and semi-synthetic endo-peroxides involves ros-dependent depolarization of the membrane potential. *The Journal of Antimicrobial Chemo-therapy* **69**: 1005-1016.

Bagar, T., Altenbach, K., Read, N.D. & Bencina, M. (2009). Live-cell imaging and measurement of intracellular pH in filamentous fungi using a genetically encoded ratiometric probe. *American Society for Microbiology* **8**: 703-712.

Bei, A.K., DeSimone, T.M., Badiane, A.S., Ahouidi, A.D., Dieye, T., Ndiaye, D., Sarr, O., Ndir, O., Mboup, S. & Duraisingh, M.T. (2010). A flow cytometry-based assay for measuring invasion of red blood cells by *Plasmodium falciparum*. *American Journal of Hematology* **85**(4): 234-237.

Bridgford, J.L., Xie, S.C., Cobbold, S.A., Pasaje, C.F.A., Herrmann, S., Yang, T., Gillett, D.L., Dick, L.R., Ralph, S.A., Dogovski, C., Spillman, N.J. & Tilley, L. (2018). Artemisinin kills malaria parasites by damaging proteins and inhibiting the proteasome. *Nature Communications* **9**(1): 1-9.

Bhisutthibhan, J. & Meshnick, S.R. (2001). Immunoprecipitation of [3H] dihydroartemisinin translationally controlled tumor protein (TCTP) adducts from *Plasmodium falciparum*-infected erythrocytes by using anti-TCTP antibodies. *Antimicrobial Agents and Chemotherapy* **45**(8): 2397-2399.

Chotivanich, K., Tripura, R., Das, D., Yi, P., Day, N.P.J., Pukrittayakamee, S., Chuor, C.M., Socheat, D., Dondorp, A.M. & White, N.J. (2014). Laboratory detection of artemisinin-resistant *Plasmodium falciparum*. *Antimicrobial Agents and Chemotherapy* **58**(6): 3157-3161.

del Pilar Crespo, M., Avery, T.D., Hanssen, E., Fox, E., Robinson, T.V., Valente, P., Taylor, D.K. & Tilley, L. (2008). Artemisinin and a series of novel endoperoxide antimalarials exert early effects on digestive vacuole morphology. *Antimicrobial Agents and Chemotherapy* **52**(1): 98-109.

Dondorp, A.M., Nosten, F., Yi, P., Das, D., Phyo, A.P., Tarning, J., Lwin, K.M., Ariey, F., Hanpithakpong, W., Lee, S.J., Ringwald, P., Silamut, K., Imwong, M., Chotivanich, K., Lim, P., Herdman, T., An, S.S., Yeung, S., Singhasivanon, P., Day, N.P.J., Lindegardh, N., Socheat, D. & White, N.J. (2009). Artemisinin resistance in *Plasmodium falciparum* malaria. *The New England Journal of Medicine* **361**(5): 455-467.

Dondorp, A.M., Yeung, S., White, L., Nguon, C., Day, N.P., Socheat, D. & von Seidlein, L. (2010). Artemisinin resistance: current status and scenarios for containment. *Nature Review Microbiology* **8**(4): 272-280.

Enserink, M. (2010). Malaria's drug miracle in danger. *Science* **328**(5980): 844-846.

Eastman, R.T. & Fidock, D.A. (2009). Artemisinin-based combination therapies: A vital tool in efforts to eliminate malaria. *Nature Review Microbiology* **7**(12): 864-874.

Eckstein-Ludwig, U., Webb, R.J.I., van Goethem, D.A., East, J.M., Lee, A.G., Kimura, M., O'Neill, P.M., Bray, P.G., Ward, S.A. & Krishna, S. (2003). Artemisinins target the SERCA of *Plasmodium falciparum*. *Nature* **424**(6951): 957-961.

Eriksson, I., Ollinger, K. & Appelqvist, H. (2017). Analysis of Lysosomal pH by Flow Cytometry Using FITC-Dextran Loaded Cells. *Methods in Molecular Biology* **1594**: 179-189.

Fairhurst, R.M. & Dondorp, A.M. (2016). Artemisinin-resistant *Plasmodium falciparum* malaria. *Microbiology Spectrum* **4**(3): 1-16.

Goldberg, D.E. (2005). Hemoglobin degradation. *Current Topic of Microbiology and Immunology* **295**: 275-291.

Guo, Z. (2016). Artemisinin anti-malarial drugs in China. *Acta Pharmaceutica Sinica B* **6**(2): 115-124.

Gruring, C., Heiber, A., Kruse, F., Ungefehr, J., Gilberger, T.-W. & Spielmann, T. (2011). Development and host cell modifications of *Plasmodium falciparum* blood stages in four dimensions. *Nature Communications* **2**(165): 1-11.

Grimberg, B.T., Erickson, J.J., Sramkoski, R.M., Jacobberger, J.W. & Zimmerman, P.A. (2008). Monitoring *Plasmodium falciparum* growth and development by UV flow cytometry using an optimized Hoechst-thiazole orange staining strategy. *Cytometry Part A* **73**(6): 546-554.

Han, J. & Burgess, K. (2010). Fluorescent indicators for intracellular pH. *Chemical Reviews* **110**: 2709-2728.

Hanboonkunupakarn, B. & White, N.J. (2016). The threat of artemisinin resistant malaria in Southeast Asia. *Travel Medicine and Infectious Disease* **14**(6): 548-550.

Hartwig, C.L., Rosenthal, A.S., D'Angelo, J., Griffin, C.E., Posner, G.H. & Cooper, R.A. (2009). Accumulation of artemisinin trioxane derivatives within neutral lipids of *Plasmodium falciparum* malaria parasites is endoperoxide-dependent. *Biochemical Pharmacology* **77**: 322-336.

Hayashi, M., Yamada, H., Mitamura, T., Horii, T., Yamamoto, A. & Moriyama, Y. (2000). Vacuolar H^+-ATPase localized in plasma membranes of malaria parasite cells, *Plasmodium falciparum*, is involved in regional acidification of parasitized erythrocytes. *The Journal of Biological Chemistry* **275**(44): 34353-34358.

Hayward, R., Saliba, K.J. & Kirk, K. (2006). The pH of the digestive vacuole of *Plasmodium falciparum* is not associated with chloroquine resistance. *Journal of Cell Science* **119**: 1016-25.

Ibrahim, N. & Abu Bakar, N. (2019). Measurement of pH of the digestive vacuole isolated from the *Plasmodium falciparum*-infected erythrocyte by digitonin permeabilization. *International Journal of Pharmaceutical Sciences and Research* **10**(5): 2587-2593.

Ismail, H.M., Barton, V., Phanchana, M., Charoensutthivarakul, S., Wong, M.H.L., Hemingway, J., Biagini, G.A., O'Neill, P.M. & Ward, S.A. (2016). Artemisinin activity-based probes identify multiple molecular targets within the asexual stage of the malaria parasites *Plasmodium falciparum* 3D7. *Proceedings of the National Academy of Sciences of the United States of America* **113**(8): 2080-2085.

Josling, G.A. & Llinas, M. (2015). Sexual development in *Plasmodium* parasites: knowing when it's time to commit. *Nature Reviews Microbiology* **13**(9): 573-587.

Klonis, N., Crespo-Ortiz, M.P., Bottova, I., Abu-Bakar, N., Kenny, S., Rosenthal, P.J. & Tilley, L. (2011). Artemisinin activity against *Plasmodium falciparum* requires hemoglobin uptake and digestion. *Proceedings of the National Academy of Sciences of the United States of America* **108**(28): 11405-11410.

Kuhn, Y., Rohrbach, P. & Lanzer, M. (2007). Quantitative pH measurements in *Plasmodium falciparum*-infected erythrocytes using pHluorin. *Cellular Micrbiology* **9**(4): 1004-13.

Li, J. & Zhou, B. (2010) Biological actions of artemisinin: Insights from medicinal chemistry studies. *Molecules* **15**(3): 1378-1397.

Marchesini, N., Luo, S., Rodrigues, C.O., Moreno, S.N.J. & Docampo, R. (2000). Acidocalcisomes and a vacuolar H+-pyrophosphatase in malaria parasites. *Biochemal Journal* **347**: 243-253.

Marchetti, A., Lelong, E. & Cosson, P. (2009). A measure of endosomal pH by flow cytometry in *Dictyostelium*. *BMC Research Notes* **2**: 7-15.

Mohd-Zamri, N.H., Mat-Desa, N.W. & Abu-Bakar, N. (2017). Sensitivity of artemisinin towards different stages of development of the malaria parasite, *Plasmodium falciparum*. *Tropical Biomedicine* **34**(4): 759-769.

Moorthy, V. & Hill, A.V.S. (2018). Malaria vaccines. *British Medical Bulletin* **62**: 59-72.

Pandey, N. & Pandey-Rai, S. (2015). Updates on artemisinin: An insight to mode of actions and strategies for enhanced global production. *Protoplasma* **253**: 15-30.

Saliba, K.J. & Kirk, K. (1999). pH regulation in the intracellular malaria parasite, *Plasmodium falciparum*. *The Journal of Biological Chemistry* **274**(47): 33213-33219.

Saliba, K.J., Allen, R.J.W., Zissis, S., Bray, P.G., Ward, S.A. & Kirk, K. (2003). Acidification of the malaria parasite's digestive vacuole by a H$^+$-ATPase and a H$^+$-pyrophosphatase. *The Journal of Biological Chemistry* **278**(8): 5605-5612.

Schalkwyk, D.A.V., Saliba, K.J., Biagini, G.A., Bray, P.G. & Kirk, K. (2013). Loss of pH control in *Plasmodium falciparum* parasites subjected to oxidative stress. *Plos One* **8**(3): e58933.

Schalkwyk, D.A.V., Chan, X.W.A., Misiano, P., Gagliardi, S., Farina, C. & Saliba, K.J. (2010). Inhibition of *Plasmodium falciparum* pH regulation by small molecule indole derivatives results in rapid parasite death. *Biochemical Pharmacology* **79**: 1291-1299.

Segami, S., Asaoka, M., Kinoshita, S., Fukuda, M., Nakanishi, Y. & Maeshima, M. (2018). Biochemical, structural, physiological characteristics of vacuolar H$^+$-pyrophosphatase. *Plant and Cell Physiology* **59**(7): 1300-1308.

Sullivan, D.J. (2013). *Plasmodium* drug targets outside the genetic control of the parasite. *Current Pharmaceutical Design* **19**(2): 282-289.

Smilkstein, M., Sriwilaijaroen, N., Kelly, J.X., Wilairat, P. & Riscoe, M. (2004). Simple and inexpensive fluorescence-based technique for high-throughput anti-malarial drug screening. *Antimicrobial Agents and Chemotherapy* **48**(5): 1803-1806.

Zhang, S. & Gerhard, G.S. (2008). Heme activates artemisinin more efficiently than hemin, inorganic iron, or hemoglobin. *Bioorganic & Medicinal Chemistry* **16**: 7853-7861.

Wang, J., Zhang, C., Chia, W.N., Loh, C.C.Y., Li, Z., Lee, Y.M., He, Y., Yuan, L., Lim, T.K., Liu, M., Liew, C.X., Lee, Y.Q., Zhang, J., Lu, N., Lim, C.T., Hua, Z., Liu, B., Shen, H., Tan, K.S.W. & Qingsong Lin. (2015). Haem-activated promiscuous targeting of artemisinin in *Plasmodium falciparum*. *Nature Communications* **6**(1): 10111-10122.

World Health Organization (2010). Global report on antimalarial drug efficacy and drug resistance: 2000–2010. Retrieved March, 03, 2019, from https://www.who.int/malaria/publications/atoz/9789241500470/en/

World Health Organization (2018). World Malaria Report 2018. Retrieved December, 12, 2018, from https://www.who.int/malaria/publications/world-malaria-report-2018/en/.

Xie, S.C., Dogovski, C., Kenny, S., Tilley, L. & Klonis, N. (2014). Optimal assay design for determining the *in vitro* sensitivity of ring stage *Plasmodium falciparum* to artemisinin. *International Journal for Parasitology* **44**(12): 893-899.